23rd ABCM International Congress of Mechanical Engineering
December 6-11, 2015, Rio de Janeiro, RJ, Brazil

# Analysis of stereolytograpghy process using a finite elements approach

[1] [2] **Marlon Wesley Machado Cunico, Ph.D. , marloncunico@usp.br**
[2]**Miriam Machado Cunico,Ph.D.**
[1]**Jonas de Carvalho, Ph.D.**
[1]Universidade de São Paulo campus São Carlos
[2]Concep3d Pesquisas Científicas

***Abstract:***
*In spite of the popularization of additive manufacturing in the past years, stereolithography process are still complex,hard to optimize, and in several cases imply on dimensional distortion and warpening because of material shrinkage during the curing phase. For that reason, the current work purpose is the analyses of stereolithography process using a finite element method. In this work, the finite element method is introduced and the interaction between poylmerization straight lines and between layers were analysed. In this case, the shrinkage ratio and conversion degree were studied as a function of laser intensity, raster velocity, material formulation. By the end, we indicated the suitable process parameter in order to avoid dimensional distortion and warpening.*

***Key words:*** *Additive manufacturing, Stereolithography, Finite elements method*

# 1. INTRODUCTION

The application of additive manufacturing (AM) technologies has grown up along the last years. As consequence, several researches related to new processes and applications have been performed. (GIBSON *et al.*, 2002; SANGERANO *et al.*, 2009; GIBSON, IAN *et al.*, 2010; GIBSON, I. *et al.*, 2010; KOLB *et al.*, 2011; CUNICO, M. W. M. e CARVALHO, J. D., 2013) One of these new processes is the Stereolithography and Mask projection stereolithography which bases its concept on the selective formation -polymer by the use of UV light.

Although this technology is one of the pioneers in additive manufacturing technologies, there are still several challenges to be overcome in order to improve and optimize such technology. For example, the current methods to simulate SLA processes are based on non matrix unidirectional finite elements. As consequence the computational are high and the models negligent angle of laser beam incidence on the resin (JIANG *et al.*, 2006; SHARMA, 2008). In addition, such method tend to be bounded by parameters as penetration depth and critical exposure. These parameters are hard to be correlated to polymerization kinetics and are related to only one material (JIANG *et al.*, 2006; SHARMA, 2008)..

On the other hand, models which are based on polymerization kinetics are generalized and allow us to predict the behaviour of material as a function of material components tenor, as consequence the material might be optimized (CUNICO e CARVALHO, 2011; CUNICO, M. W. M. e CARVALHO, J., 2013).

For that reason, the present work proposes a novel finite element method for the SLA simulation and the characterization of polymer formation during light exposition.

# 2. DYNAMIC FINITE ELEMENT METHOD

This finite element method was mainly divided in: energy balance, photopolymerisation kinetics, simulation management and results generation. It is important to note that this method is a new approach of selective photopolymerization simulation, as the energy balance and photopolymerization kinetics are considered in a separated steps. In addition, the diffraction of light is not considered this and other methods because of irrelevance of this parameter in SLA simulations.

In other methods which have been design for stereolithography processes, the polymerization models are mostly related to penetration depth parameter (JIANG *et al.*, 2006; SHARMA, 2008). In this approach, the understanding of physical-

chemical reaction is not clear and the coefficient determination is only defined experimentally. Therefore, the coefficient of different material formulations cannot be predicted numerically.

For that reason, the proposed model used a different approach and considers the polymerization rate as characterization parameter. It allow predicting numerically the effect of material formulation on polymerization profile. In this method, the shrinkage factor is also characterised as a function of degree of polymerization and material formulation.

In order to solve the light transmittance and energy balance, we assumed that each finite element is composed by transmittance matrix where the light inside such element occurs in longitudinal direction.

In addition, the balance of energy considers that the sum of energy inside the element must be null. That assumption can be interpreted as an expansion of Beer-Lamb Law (Eq. (1)) which considers that consider that the sum of light intensities is null in only one dimension. In Beer-Lamb Law, the absorbed light intensity ($I_{absorbed}$) is a function of input intensity ($I_{in}$), absorbance rate ($\alpha$), thickness ($l$) and substance/initiator molar concentration ([c]). As consequence, the output intensity ($I_{out}$) is the difference between input intensity ($I_{in}$) and absorbed intensity ($I_{absorbed}$) (FOUASSIER e RABEK, 1993; BRANDRUP *et al.*, 1999; ANDRZEJEWSKA, 2001; MATYJASZEWSKI e DAVIS, 2002; FOUASSIER *et al.*, 2003; LOVESTEAD *et al.*, 2003; ODIAN, 2004; BODDAPATI *et al.*, 2011).

$$I_{out} = I_{in} - I_{absorbed} = I_{in} - I_{in} \cdot e^{-\alpha \cdot l \cdot [c]} \quad \textbf{(1)}$$

Another representation for these equations can be seen in Figure 1, where a network diagram of the finite element express the energy balance in one dimension element. In this representation, the energy balance scheme in one dimension is a different approach for dynamic finite element methods of SLA processes. On the other hand, the energy balance that considers diffraction in two and 3 dimension has been proposed in this work in order to characterise the selective composite formation process.

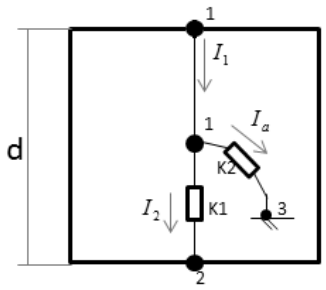


**Figure 1 – Network scheme of Energy balance in one dimension (SLA scheme)**

In this approach, the light flux is determined by the light transmittance (inverse of light resistance) and the absorbed light intensity is marked by a light flux leakage. In this case, the energy balance inside the element can be defined according to a transmittance matrix (T), light intensity flux vector (I) and a nodal light intensity difference vector (A), as presented in Eq. (2).

$$[T] \cdot [A] = [I] \quad \textbf{(2)}$$

Assuming one element example, the local energy balance equation is represented by transmittance matrix, intensity flux vector and nodal light intensity difference vector is:

$$\begin{bmatrix} K1+K2 & -K1 & -K2 \\ -K1 & K1 & 0 \\ -K2 & 0 & K2 \end{bmatrix} \cdot \begin{bmatrix} a1 \\ a2 \\ a3 \end{bmatrix} = \begin{bmatrix} I1 \\ I2 \\ Ia \end{bmatrix} \quad \textbf{(3)}$$

Therefore, it is possible to find the diffracted and absorbed light intensities after the definition of boundary conditions, input node and light intensity. In this case, the definition of the absorbed coefficient might be described as:

$$I_a = \frac{K2}{K1+K2} \cdot I_1 = I_1 \cdot e^{-\alpha \cdot l \cdot [c]} \quad \textbf{(4)}$$

$$K2 = \frac{K1 \cdot e^{-\alpha \cdot l \cdot [c]}}{\left(1 - e^{-\alpha \cdot l \cdot [c]}\right)} \quad \textbf{(5)}$$

And considering that the initiator concentration is proportional to the monomer amount, we can indicate the absorption coefficient as a function of the degree of polymer conversion as:

$$K2 = \frac{K1 \cdot e^{-\alpha \cdot l \cdot [c] \cdot (1-P)}}{\left(1 - e^{-\alpha \cdot l \cdot [c] \cdot (1-P)}\right)} \quad \textbf{(6)}$$

One of the main approaches to characterise the photopolymerisation kinetics is the polymerization rate (RP), Eq (7). This parameter indicates the variation of monomer concentration or the carbon double bonds as a function of time (t), where the main variables are the monomer concentration (M) or carbon double bond ($[C=C]$), absorbed light intensity ($I_a$), quantum yield of initiation or quantum efficiency ($\phi$). In addition, kp is the constant of propagation and kt is the constant of termination (JACOBS, 1992; FOUASSIER e RABEK, 1993; BRANDRUP *et al.*, 1999; ANDRZEJEWSKA, 2001; MATYJASZEWSKI e DAVIS, 2002; SANGERMANO *et al.*, 2002; MARPLE e LOWDER, 2003; HAGUE *et al.*, 2004; ODIAN, 2004; ZHIWEI *et al.*, 2006; VOLPATO, 2007; LI *et al.*, 2009; GIBSON, IAN *et al.*, 2010; HUANG *et al.*, 2010; CUNICO, 2011).

$$Rp = \frac{-d[M]}{dt} = \frac{kp}{\sqrt{kt}} \cdot [M] \cdot (\phi \cdot I_a)^{1/2} = \frac{kp}{\sqrt{kt}} \cdot [C=C] \cdot (\phi \cdot I_a)^{1/2} \quad \textbf{(7)}$$

Therefore, the degree of conversion ([P]) might be identified by the integration of polymerization with the time, as presented in Eq. (8) (ANDRZEJEWSKA, 2001; WATTS, 2005).

$$[P] = \frac{1}{[M_0]} \cdot \int_0^t Rp \cdot dt = \frac{1}{[M_0]} \cdot \int_0^t \frac{-d[M]}{dt} \cdot dt = 1 - (1 - [P_0]) \cdot e^{-\frac{kp}{\sqrt{kt}} \cdot (\phi \cdot I_a)^{1/2} \cdot t} \quad \textbf{(8)}$$

For the identification of shrinkage ratio, we used one numerical model that correlates the degree of conversion and the volumetric shrinkage-strain. The Eq. (9) presents a numerical model that express the volumetric shrinkage of a monomer as a function of degree of conversion ([P]), functionality of monomer ($f_i$), mole fraction of monomer ($\chi_i$), molecular mass of monomer ($M_i$) and density of mixture ($\rho_{mix}$).

$$\frac{\Delta V}{V}(\%) = 22.5 \cdot [P] \cdot \frac{\sum_i f_i \cdot \chi_i}{\sum_i M_i \cdot \chi_i} \cdot \rho_{mix} \cdot 100 \quad \textbf{(9)}$$

For the management of simulation, we developed a routine which concerns data input; mesh generation; time discretisation; transient light exposure, energy balance calculation; results calculation (polymer conversion and layer adherence ratio); and layer construction as it is presented in Figure 2.

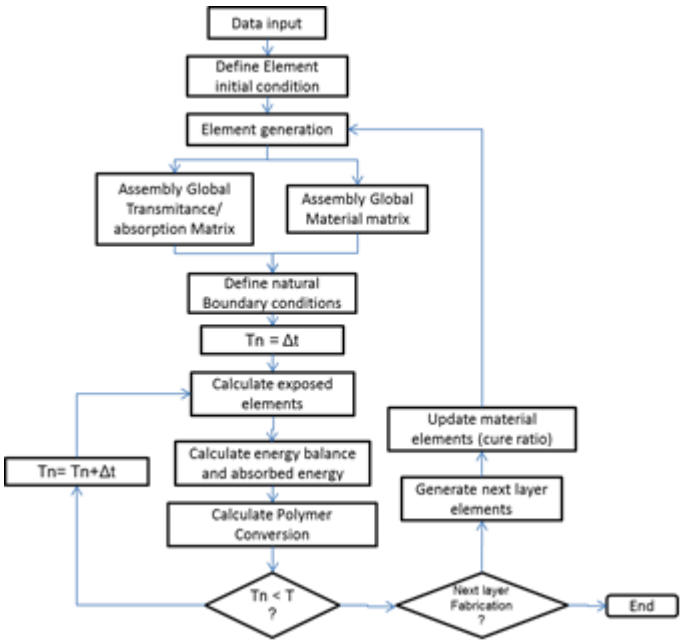


**Figure 2 – Schematic of simulation management**

# 3. MATERIAL AND METHODS

In order to analyse the behaviour of polymer formation, we defined 4 study cases which investigated the polymerization profile of a single straight polymerization line in addition to the interaction between polymerization lines and interaction between layers. Either study cases were analysed in the transversal section of line formation direction in order to evidence the degree of polymer conversion, shrinkage ratio and lack of adherence between layers.

The essential parameters that were defined in the finite elements methods are simulation time step (for transient-state analysis), study region size and mesh size.

In this study, the initial study region was 3x1x1mm, and for each new layer, the study region was updated and increased in z direction according to the layer thickness. We have also used hexahedron elements shape where the main dimensions are 5x5x5μm. By the end, we used 0.01 seconds of time-step in order to identify the dynamic behaviour of photopolymerisation and composite formation profile.

After defined the finite element method, we have selected an analysis condition and experimentally identified the main models coefficients related to photopolymeric material. In this analysis condition, the main properties of these materials were characterised, as such polymerisation rate of resin formulation.

In this study, we considered a photopolymeric material based on acrylates where the main formulation compounds were monomer, oligomer and photoinitiator. In this case, *methyl methacrylate* (MMA) was the monomer (M) (SIGMA-ALDRICH, 2008a), *Trimethylopropane triacrylate* (TMPTA) (SIGMA-ALDRICH, 2008b) was the oligomer (O) or crosslink agent and the Omnirad 2500 was the photoinitiator (PI) (IGM, 2005). We have also defined the ratio between monomer and oligomer as 2 and the photoinitiator concentration as 0.2% wt.

With respect to the simulated process parameters, we established constant values for laser intensity, laser beam diameter, laser beam light wave length, laser beam intensity distribution (Gaussian), raster velocity, distance between polymerisation lines, number of analysed lines, layer thickness and number of analysed layers. Table 1 presents the relation of these parameters and their values.

With respect to the simulated process parameters, we established constant values for laser intensity, laser beam diameter, laser beam light wave length, laser beam intensity distribution (Gaussian), raster velocity, distance between polymerisation lines, number of analysed lines, layer thickness and number of analysed layers. Table 1 presents the relation of these parameters and their values.

**Table 1 – Relation of main process parameters used in the numerical simulation**

| | Case 1 | Case 2 | Case 3 | Case 4 |
|---|---|---|---|---|
| Number of layers | 1 | 1 | 2 | 2 |
| Number of lines | 1 | 2 | 1 | 2 |
| Laser Intensity | 100 mW | | | |
| Laser beam Diameter | 0,6 mm | | | |
| Laser beam light wave length | 378 nm | | | |
| Raster velocity | 25 mm/s | | | |
| Distance between polymerization lines | 0,8 mm | | | |
| Layer thickness (substrate) (mm) | 0,15 mm | | | |

By the end, we have implemented the finite element method in a Matlab code, where a penalty method was used to apply the essential boundary conditions and solve the light transmittance matrix (DEB, 2006).

# 4. RESULTS AND DISCUSSIONS

As result of the proposed method, we were able to identify the polymerization gradient as a function of laser beam intensity, raster velocity, and distance between layer and polymerization lines.

In Figure 3, a simulation result is presented where polymerization profile is presented for one line of polimerization and one layer. It is possible to see that the penetration follows a parable shape as result of laser beam Gausian intensity distribuition.

In this figure, the degree of polimerization is presented in a transversal section where the maximum polymerization degree was found to be 65%.

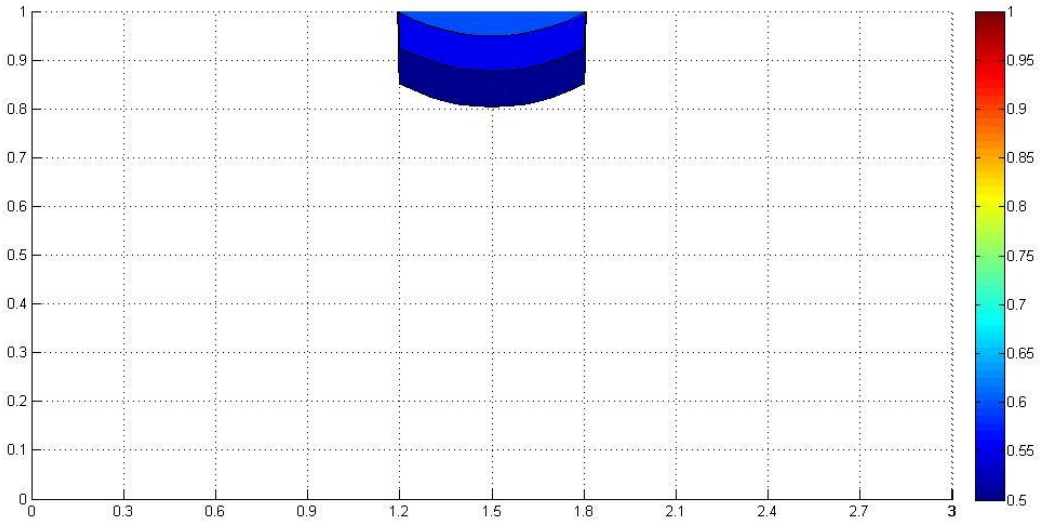


**Figure 3 – Result of polymerization profile considering 1 polymerization line and 1 layer**

Otherwise, the analysis of 2 queued layers (Figure 4) indicated a peak of polymerization, which is resulted by the cumulative effect and overlap between layers.

In this case, it is possible to see that although the new layer is about to be formed, the previous layers was also modified, increasing the penetration.

This situation reflects the how important is the penetration depth, which is an important property that indicates and ensure the maximum distortion that a previous layer might suffer.

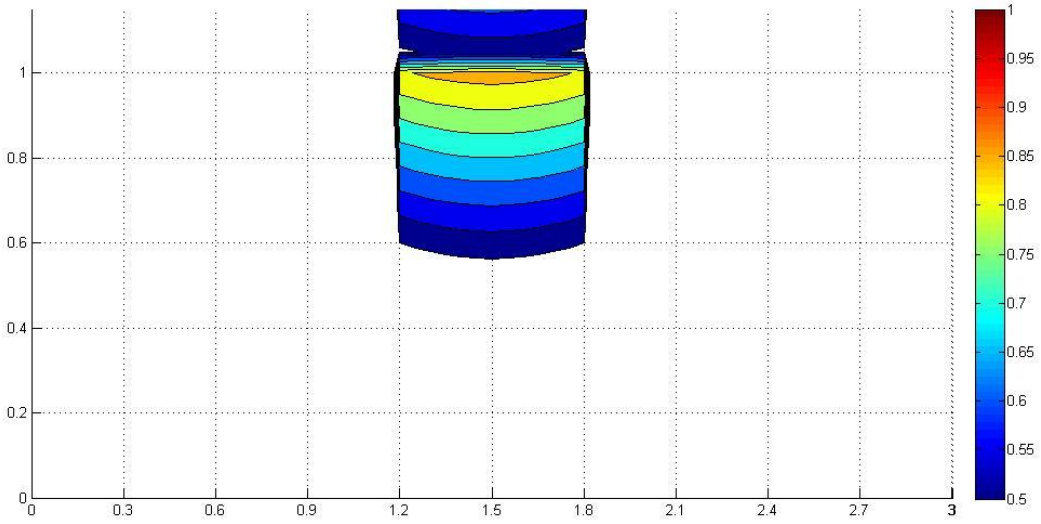


**Figure 4 – Result of polymerization profile considering 1 polymerization line and 2 layer**

In spite of that, when we simulated 6 queue layers, a polymerized area with more than 65% of polymer conversion was found.

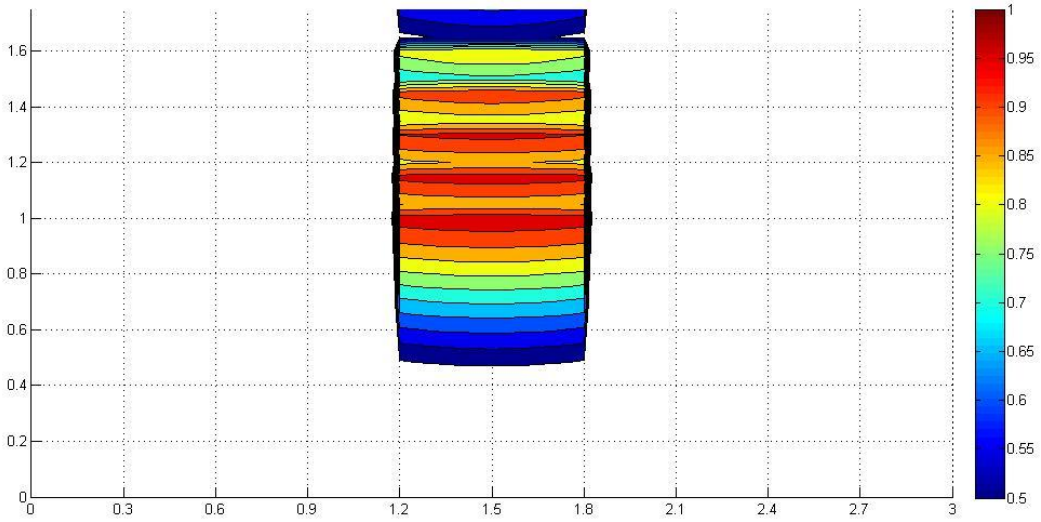


**Figure 5 – Result of polymerization profile considering 1 polymerization line and 2 layer**

Analysing the simulation of 2 polymerization lines in one and two layer (Figure 6 and Figure 7), we could identify that the profile of polymerization remained similar to the previous study cases. Nevertheless, it was possible to see that such method is possible to simulate additive manufacturing processes which are based on UV curable resins.

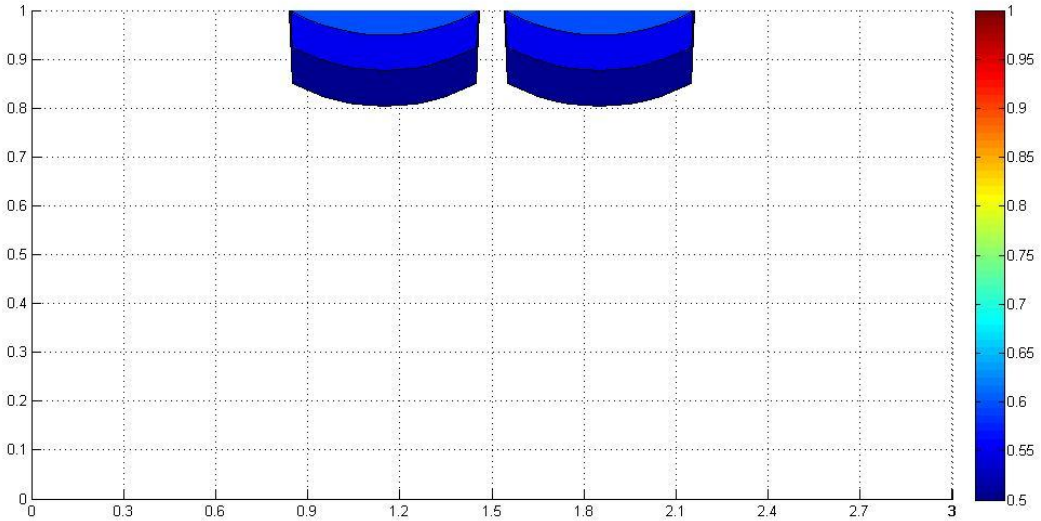


**Figure 6 – Result of polymerization profile considering 2 polymerization line and 1 layer**

In addition, besides manufacturing issues like warpening and stress concentration might be prevented, the process might be optimized as a function of process strategy, resin properties and equipment parameters.

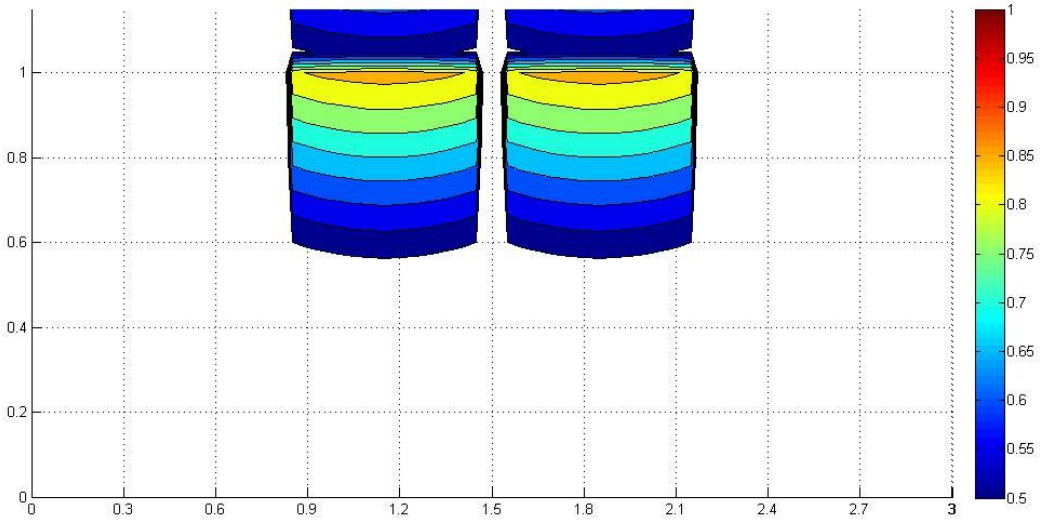


**Figure 7 – Result of polymerization profile considering 2 polymerization line and 2 layer**

# 5. CONCLUSIONS

Along this work, a novel dynamic finite element method was presented and the simulations of some simple cases were exposed.

In this study, it was included new concepts to calculate polymerization profile in SLA processes which is found to be more generalized than current methods.

Along this study, the profile of polymerization was seen to be parabolic as expected, even though previous layers was found to be affected by the formation of new layers.

This method also proof to be useful to determine stress concentration and simulate manufacturing distortion.

However, as this work is still in the preliminary stage further investigations are needed to identify the potential of method and evaluate the accuracy of such methods in comparison with experimental studies.

# 6. ACKNOWLEDGMENTS

The authors would like to thank the CNPQ for financial support, as well as the Department of Mechanical Engineering of the University of São Paulo,(campus São Carlos) and the research department of Concep3D for providing access to infrastructure and Laboratories.

# 7. REFERENCES

ANDRZEJEWSKA, E. Photopolymerization kinetics of multifunctional monomers. **Progress in Polymer Science**, v.26, n.4, p.605-665. 2001.

BODDAPATI, A., S. B. RAHANE, *et al.* Gel time prediction of multifunctional acrylates using a kinetics model. **Polymer**, v.52, n.3, p.866-873. 2011.

BRANDRUP, J., E. H. IMMERGUT, *et al.*, Eds. **Polymer Handbook**: John Wiley & Sons, Inc., p.2370 ed. 1999.

CUNICO, M. M. W. M. Development of New Rapid Prototyping Process. **Rapid Prototyping Journal**, v.17, n.2, p.6-6. 2011.

CUNICO, M. W. M. e J. CARVALHO. OPTIMIZATION OF RAPID PROTOTYPING PROCESS BASED ON SIMULTANEOUS DEPOSITION AND PHOTOPOLYMERIZATION USING ANALYTIC APPROACH. **21st INTERNATIONAL CONGRESS OF MECHANICAL ENGINEERING, 2011**. Natal: ABCM 2011.

CUNICO, M. W. M. e J. CARVALHO. Optimization of thick layers photopolymerization systems and analytical aproach. **Rapid prototyping journal**. 2013.

CUNICO, M. W. M. e J. D. CARVALHO. OPTIMIZATION OF POSITIONING SYSTEM OF FDM MACHINE DESIGN USING ANALYTICAL APROACH. **Rapid Prototyping Journal**, v.19, n.3. 2013.

DEB, D. **Finite Element Method: Concepts and Applications in Geomechanics**: Prentice-Hall of India. 2006. 269 p.

FOUASSIER, J., X. ALLONAS, *et al.* Photopolymerization reactions under visible lights: principle, mechanisms and examples of applications. **Progress in Organic Coatings**, v.47, n.1, p.16-36. 2003.

FOUASSIER, J. P. e J. RABEK. **Radiation Curing in Polymer Science and Technology: Fundamentals and Methods**. London: Springer. 1993. 563 p.

GIBSON, I., T. KVAN, *et al.* Rapid prototyping for architectural models. **Rapid Prototyping Journal**, v.8, n.2, p.91-95. 2002.

GIBSON, I., D. W. ROSEN, *et al.* **Additive Manufacturing Technologies: Rapid Prototyping to Direct Digital Manufacturing**: Springer. 2010. 473 p.

GIBSON, I., D. W. ROSEN, *et al.* Photopolymerization Processes. In: (Ed.). **Additive Manufacturing Technologies**: Springer US, 2010. Photopolymerization Processes, p.61-102

HAGUE, R., S. MANSOUR, *et al.* Materials analysis of stereolithography resins for use in Rapid Manufacturing. **Journal of materials science**, v.39, n.7, p.2457-2464. 2004.

HUANG, B., J. MO, *et al.* The properties of an UV curable support material pre-polymer for three dimensional printing. **Journal of Wuhan University of Technology--Materials Science Edition**, v.25, n.2, p.278-281. 2010.

IGM. Omnirad CureAll 2500 Photo-initiator Compound. IGM Resins - UV Radcure Specialities. 2005. Disponível em: <www.igmresins.com/>. Acesso em: agosto de 2011.

JACOBS, P. F. **Rapid Prototyping & Manufacturing: Fundamentals of SteroLithography**: Society of Manufacturing Engineers. 1992. 434 p.

JIANG, C.-P., Y.-M. HUANG, *et al.* Dynamic finite element analysis of photopolymerization in stereolithography. **Rapid Prototyping Journal**, v.12, n.3, p.173-180. 2006.

KOLB, E., C. KUMMERLÖWE, *et al.* Characterization of a nanoparticle-filled resin for application in scan-LED-technology. **Journal of Materials Science: Materials in Medicine**, v.22, n.10, p.2165-2173. 2011.

LI, H., L. ZHANG, *et al.* UV curing behavior of a highly branched polycarbosilane. **Journal of Materials Science**, v.44, n.4, p.970-975. 2009.

LOVESTEAD, T. M., A. K. O'BRIEN, *et al.* Models of multivinyl free radical photopolymerization kinetics. **Journal of Photochemistry and Photobiology A: Chemistry**, v.159, n.2, p.135-143. 2003.

MARPLE, M. G. e S. B. LOWDER. UV cure resin molding method. United States: Lowder, Scott Byerley 2003.

MATYJASZEWSKI, K. e T. P. DAVIS, Eds. **Handbook of Radical Polymerization**: John Wiley and Sons, Inc., Hoboken., p.935 ed. 2002.

ODIAN, G. **Principles of Polymerization**: John Wiley & Sons, Inc. 2004. 840 p.

SANGERANO, M., E. PALLARO, *et al.* UV-cured epoxy coating reinforced with sepiolite as inorganic filler. **Journal of Materials Science**, v.44, n.12, p.3165-3171. 2009.

SANGERMANO, M., G. MALUCELLI, *et al.* Coatings obtained through cationic UV curing of epoxide systems in the presence of epoxy functionalized polybutadiene. **Journal of materials science**, v.37, n.22, p.4753-4757. 2002.

SHARMA, P. **Numerical Analysis Of Stereolithography Process Using The Finite Element Method**. THAPAR UNIVERSITY, 2008.

SIGMA-ALDRICH. Methyl Methacrylate, 99%. Sigma-Aldrich Co. 2008a. Disponível em: <http://www.sigmaaldrich.com/catalog/search/ProductDetail/ALDRICH/M55909>. Acesso em: agosto de 2011.

_____. Trimethylolpropane triacrylate. Sigma-Aldrich Co. 2008b. Disponível em: <http://www.sigmaaldrich.com/catalog/search/ProductDetail/ALDRICH/246808>. Acesso em: agosto de 2011.

VOLPATO, N., Ed. **Prototipagem Rápida : Tecnologias e Aplicações**: EDGARD BLUCHER, p.272, 1st ed. 2007.

WATTS, D. C. Reaction kinetics and mechanics in photo-polymerised networks. **Dental Materials**, v.21, n.1, p.27-35. 2005.

ZHIWEI, G., M. JIANHUA, *et al.* Development of a hybrid photopolymer for stereolithography. **Journal of Wuhan University of Technology--Materials Science Edition**, v.21, n.1, p.99-101. 2006.